Science Advances

AAAS

advances.sciencemag.org/cgi/content/full/3/12/eaap8576/DC1

Supplementary Materials for

Optimization principles and the figure of merit for triboelectric generators

Jun Peng, Stephen Dongmin Kang, G. Jeffrey Snyder

Published 15 December 2017, *Sci. Adv.* **3**, eaap8576 (2017)
DOI: 10.1126/sciadv.aap8576

This PDF file includes:

The Ideal Model

The ideal model can be described with a circuit diagram as shown in fig. S1a. $-S\sigma$ is the triboelctrically produced surface charge on the dielectric layer that is maintained at a steady value over time. On the metal side an opposite charge $S\sigma$ is initially established (*i.e.* $Q(t=0)=0$ in fig. S1a). The metal-dielectric distance (air gap) changes sinusoidally over time

$$x(t) = x_{\max} \cdot \frac{(1-\cos\omega t)}{2} \tag{S1}$$

which induces a change in the air-gap contribution of the capacitance

$$\frac{1}{C(t)} = \frac{x(t)}{S\epsilon_0} = \frac{x_{\max}}{S\epsilon_0}\frac{(1-\cos\omega t)}{2} = \frac{1}{C_{\text{air}}}\frac{(1-\cos\omega t)}{2} \tag{S2}$$

Here C_{air} was defined as the air-gap contribution of the capacitance at $x = x_{\max}$. C_{device} is the capacitance of the device that remains constant over time, including the contribution from the dielectric layer and any additional capacitors connected in series to the dielectric layer. R_L is the load resistance.

The time-varying $C(t)$ drives charge $Q(t)$ from the moving electrode to the stationary electrode, making the moving electrode charge $S\sigma - Q(t)$ and the stationary electrode charge $Q(t)$. We can use Kirchhoff's voltage law to find the differential equation describing charge Q

$$R_{\text{L}}\frac{dQ}{dt} + Q\left(\frac{1}{C_{\text{device}}} + \frac{1}{C(t)}\right) - \frac{S\sigma}{C(t)} = 0 \tag{S3}$$

To reduce the differential equation to a dimensionless form, we define reduced parameters. The mechanical driving motion is reduced to $x^* \equiv x(t)/x_{\max}$ and instead of time we use phase angle $\theta = \omega t$. Since charge Q is always a fraction of $S\sigma$, we define $Q^* = Q/S\sigma$. The two independent parameters are the dimensionless resistance

$$R^* \equiv \omega R_L C_{\text{air}} = \frac{R_L \omega \epsilon_0 S}{x_{\max}} \tag{S4}$$

and the dimensionless device capacitance

$$C^* \equiv \frac{C_{\text{device}}}{C_{\text{air}}} \tag{S5}$$

Differential equation Eq.S3 then reduces to

$$R^* \frac{dQ^*}{d\theta} + Q^* \left(\frac{1}{C^*} + x^* \right) = x^* \tag{S6}$$

By using the integration factor method, the analytical solution of Q^* can be obtained for the initial condition of $Q^*(0) = 0$

$$Q^*(\theta) = \frac{\int_0^\theta (1-\cos t) \cdot \exp\left[\frac{1}{2R^*} \left(\frac{2t}{C^*} + t - \sin t \right) \right] dt}{2R^* \exp\left[\frac{1}{2R^*} \left(\frac{2\theta}{C^*} + \theta - \sin\theta \right) \right]} \tag{S7}$$

Since our prime interest is in the steady state where $Q(\theta) = Q(\theta + 2\pi)$, we can use this condition to replace the integral in Eq.S7 with one that runs over only one period

$$Q^*_{\text{steady}}(\theta) = \frac{\exp\left(\frac{\sin\theta}{2R^*} \right)}{2R^* \left(\exp\left[\frac{\pi}{R^*} \left(\frac{2}{C^*} + 1 \right) \right] - 1 \right)} \int_0^{2\pi} [1 - \cos(t+\theta)] \cdot \exp\left[\frac{1}{2R^*} \left(\frac{2t}{C^*} + t - \sin(t+\theta) \right) \right] dt \tag{S8}$$

Using Q^*, we can also define dimensionless current (I^*), voltage (V^*), and power (P^*)

$$I^* \equiv \frac{dQ^*}{d\theta} \tag{S9}$$

$$V^* \equiv I^* R^* \tag{S10}$$

$$P^* \equiv I^{*2} R^* \tag{S11}$$

Real current (I), voltage (V), and power (P) is found by simply scaling the dimensionless values

$$I = I^* \cdot S\sigma\omega \tag{S12}$$

$$V = V^* \cdot \frac{\sigma x_{\max}}{\epsilon_0} \tag{S13}$$

$$P = P^* \cdot \frac{x_{\max} \sigma^2 S\omega}{\epsilon_0} \tag{S14}$$

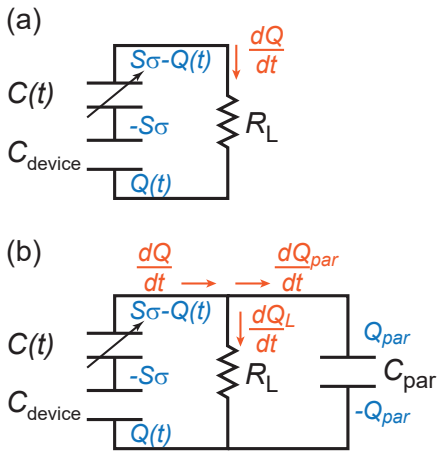

fig. S1. Circuit model diagrams of triboelectric generators.
Circuit model diagrams of the triboelectric generator for (a) the ideal model and (b) the parasitic capacitance model. Definitions of charges (blue text) and currents (orange text) are shown together on the circuit diagram. $-S\sigma$ represents the constant charge on the dielectric layer. $S\sigma - Q(t)$ and $Q(t)$ represent the charges in the moving electrode and stationary electrode, respectively.

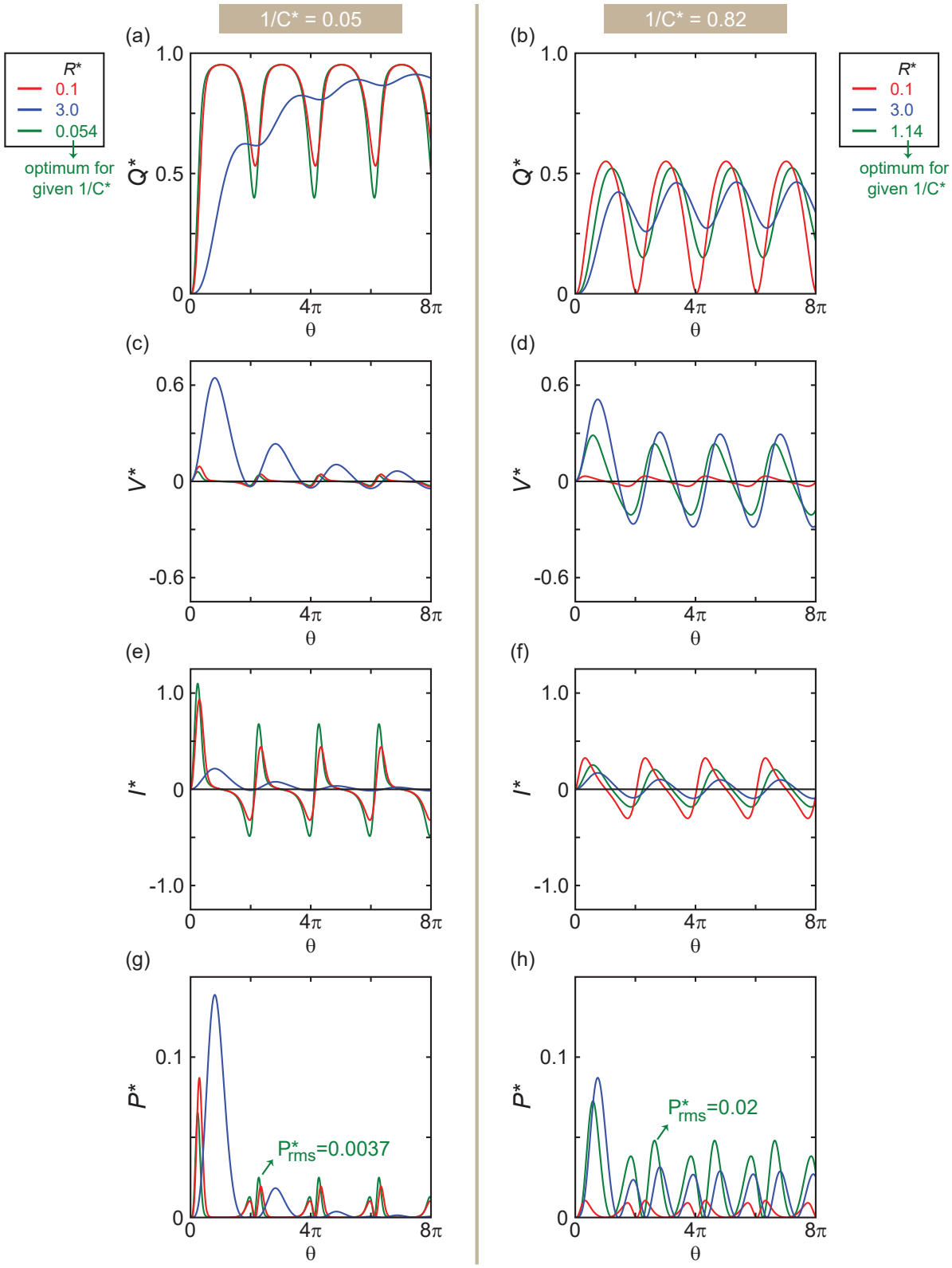

fig. S2. Transient characteristics of the ideal model. The left and right columns correspond to $1/C^* = 0.05$ and 0.82, respectively. The green lines show the optimum R^* condition for each $1/C*$, while the red and blue lines represent two non-optimal load resistances. (a-b) Q^*, (c-d) V^*, (e-f) I^*, and (g-h) P^*. It is seen that the steady-state is reached within the first two cycles in most cases except for the case with highest R^* and lowest $1/C^*$. The bad matching case ($1/C^* = 0.05$) shows sharper peaks in V^*, I^*, and P^*, whereas the good matching case ($1/C^* = 0.82$) shows smoother behavior. The resulting power after integration over θ is much higher in the good matching case. It is also seen that the first transient cycle generates more power than at steady-state, especially for high R^*. Initial conditions were set to $Q^* = 0$ in all cases.

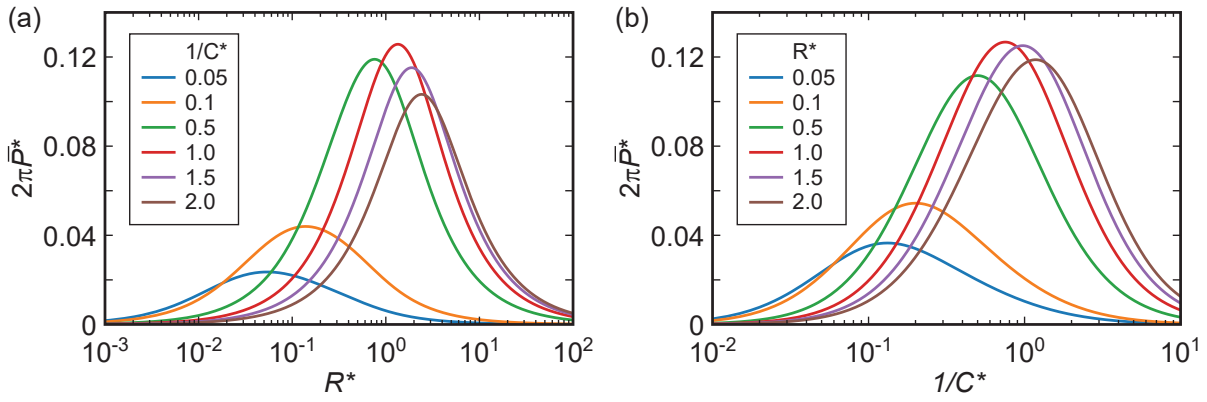

fig. S3. One-dimensional projections of the steady-state dimensionless power output. Steady-state dimensionless power output per cycle for: (a) a given $1/C^*$ and as a function of R^*; (b) a given R^* and as a function of $1/C^*$.

The transient solution for a number of example cases are plotted in fig. S2. When R^* is high, it is seen that the power during the first cycle is much higher than that of the steady-state. By comparing the two cases of $R^* = 3$ with different $1/C^*$, *i.e.* $1/C^* = 0.05$ (fig. S2g) and $1/C^* = 0.82$ (fig. S2f), it is observed that during the first cycle the bad matching case ($1/C^* = 0.05$) case has even higher power generation than the good matching case ($1/C^* = 0.82$) despite the steady-state power being orders of magnitude smaller. Therefore, modeling the transient cycle (*19*) could lead to results significantly discrepant from real device operation. In the main text, we focus our analysis on the steady-state behavior.

Figure S3 plots the steady state power output with respect to $1/C^*$ and R^*, when one is fixed and the other is varied. These plots are equivalent to vertical and horizontal cross sections of the color contour plot shown in Fig.3 of the main text.

Parasitic Capacitance Model

Parasitic capacitance is modeled by adding a capacitor in parallel to the load resistor (C_{par}) as shown in fig. S1b. Instead of Q always going through the load resistor, the charge splits to a part going through the load resistor (Q_L) and the other leaking into the parasitic capacitor (Q_{par}). From Kirchhoff's current law

$$\frac{dQ}{dt} = \frac{dQ_{\text{L}}}{dt} + \frac{dQ_{\text{par}}}{dt} \tag{S15}$$

With the initial condition $Q(t=0) = Q_L(t=0) = Q_{\text{par}}(t=0) = 0$, we obtain

$$Q = Q_L + Q_{\text{par}} \tag{S16}$$

Use of Kirchhoff's voltage law on two different loops in fig. S1b yields a set of differential equations

$$R_{\text{L}}\frac{dQ_L}{dt} + Q\left(\frac{1}{C_{\text{device}}} + \frac{1}{C(t)}\right) - \frac{S\sigma}{C(t)} = 0 \tag{S17}$$

$$R_{\text{L}}\frac{dQ_L}{dt} - \frac{Q_{\text{par}}}{C_{\text{par}}} = 0 \tag{S18}$$

We can combine Eqs.S16-S18 into a differential equation describing only Q_L

$$R_{\text{L}}\frac{dQ_L}{dt} + \left(Q_L + \frac{dQ_L}{dt}R_{\text{L}}C_{\text{par}}\right)\left(\frac{1}{C_{\text{device}}} + \frac{1}{C(t)}\right) - \frac{S\sigma}{C(t)} = 0 \tag{S19}$$

which is of our interest for analyzing power output at the load resistor. Note the additional term containing C_{par} compared with the ideal model (Eq.S3), which requires an additional independent parameter to

describe the behavior of the system. We define dimensionless parasitic capacitance

$$C^*_{\rm par} \equiv \frac{C_{\rm par}}{C_{\rm air}} \tag{S20}$$

which is the added independent parameter. We also define $Q^*_L = Q_L/S\sigma$ as we did previously for Q^*.

The dimensionless differential equation then becomes

$$R^*\frac{dQ^*_L}{d\theta} + \left(Q^*_L + \frac{dQ^*_L}{d\theta}R^*C^*_{\rm par}\right)\left(\frac{1}{C^*} + x^*\right) = x^* \tag{S21}$$

Parasitic capacitance reduces the power as shown in fig. S4. The optimum R^* and $1/C^*$ shift to smaller values; one needs to minimize the leakage current by reducing the resistance of the load. As a result, the output voltage level is compromised more than the current level (fig. S4c-d).

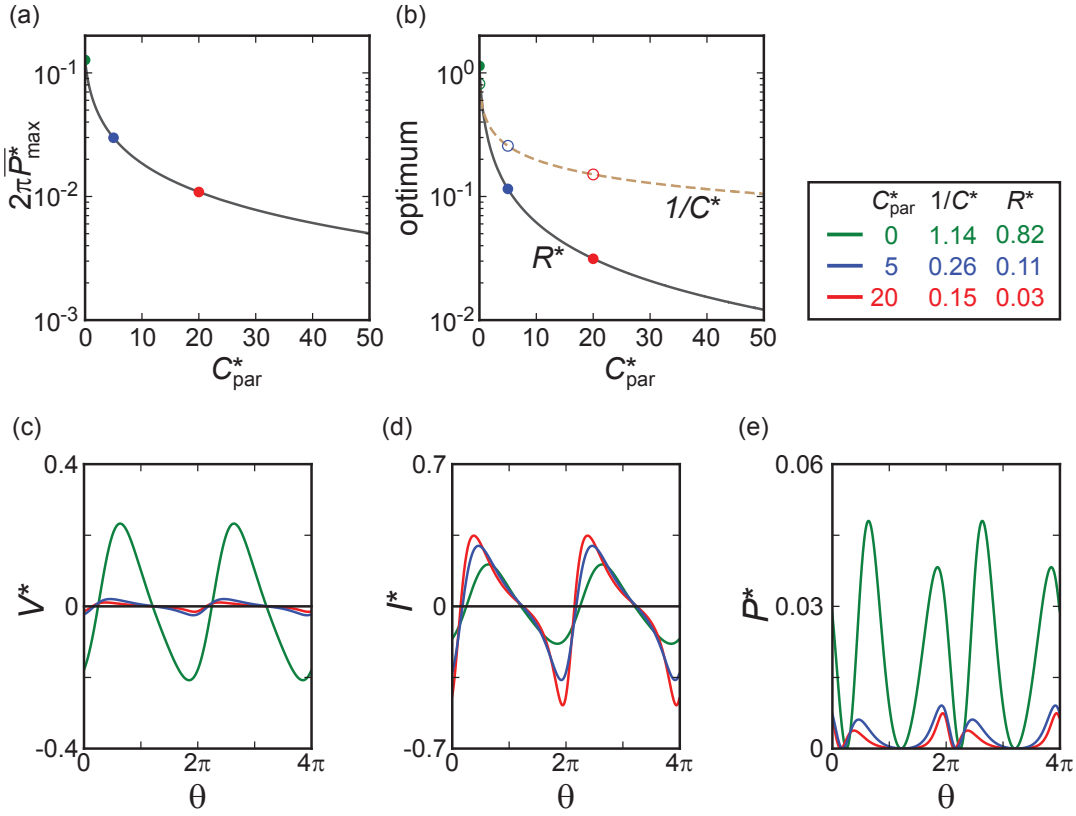

fig. S4. The influence of parasitic capacitance on device characteristics.
The influence of parasitic capacitance on (a) the maximum power generation and (b) the optimum R^* and $1/C^*$. (c) V^*, (d) I^*, and (e) P^* curves for two examples cases of $C^*_{\rm par} = 5$ and 10, compared with the ideal case with no parasitic capacitance. The optimum R^* and $1/C^*$ values for each of the example cases are given in the legend and indicated in (b). The average power of each cases is indicated in (a).

Power Output vs. Work Input

Work done by the mechanical motion, in dimensionless units identical to P^*, is

$$W^* = (1 - Q^*)^2 \cdot \frac{\sin\theta}{4} \tag{S22}$$

which can be derived by finding the force required to maintain the steady motion. We can then compare this work input to the power output as shown in fig. S5. We note that the input work is positive for the

separation process ($\theta = [0, \pi]$), but negative for the reverse process ($\theta = [\pi, 2\pi]$). When integrated over the entire cycle, the area is identical for the output and input curves which indicates 100 % conversion efficiency. This energy conversation is an expected result from the model because the load resistor is the only element that consumes power; ideal capacitors do not consume power.

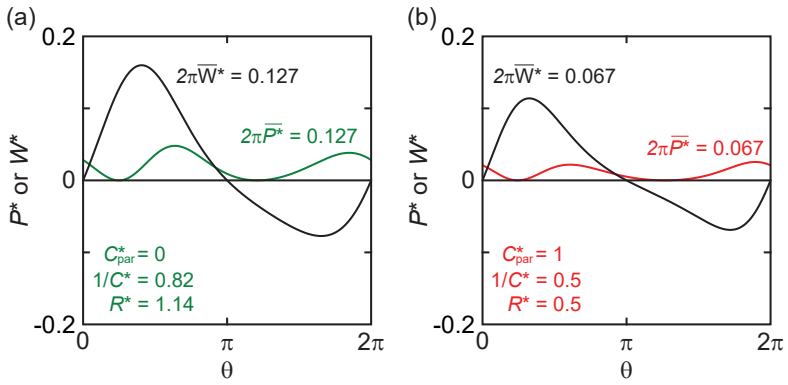

fig. S5. Comparison of the output power and mechanical work input.
Comparison of the output power and mechanical work input for (a) the global optimum condition and (b) an arbitrary non-optimal condition with finite parasitic capacitance. The integrated area of the input (W^*) and output (P^*) curves are exactly identical in both cases. The positive and negative work input is: (a) 0.282 and -0.154; (b) 0.191 and -0.123, respectively. The device parameters used for the calculation are given in the legend.